Nano Energy 67 (2020) 104284

Contents lists available at ScienceDirect

Nano Energy

journal homepage: http://www.elsevier.com/locate/nanoen

Full paper

# Effects of heat transfer and the membrane thermal conductivity on the thermally nanofluidic salinity gradient energy conversion

Rui Long *, Zuoqing Luo, Zhengfei Kuang, Zhichun Liu **, Wei Liu ***

*School of Energy and Power Engineering, Huazhong University of Science and Technology, Wuhan, 430074, PR China*

ARTICLE INFO

*Keywords:*
Energy harvesting
Nanofluidics
Thermal conductivity
Heat transfer
Membrane selection

ABSTRACT

Originating from advances in nanofabrication, functional materials have been developed to construct bioinspired or mimic nanochannels for efficient nanofluidic energy conversion. In previous studies regarding nanofluidic energy conversion, the material thermal conductivity has been never taken into consideration, however, which shall be addressed with transmembrane temperature difference applied. Thermal conductivities of widely used bulk materials for fabricating nanopores vary from 0 to 120 W/(m·K). Heat transfer occurs both in the liquid solution and solid membrane, impacting *trans*-channel solution temperature distribution and ion transportation, and yielding counterintuitive phenomena. Under positive temperature differences, the electric power shifts from inhibition to promotion as the membrane thermal conductivity increases. Larger membrane thermal conductivity evens temperature distribution in the nanochannel, weakening ion aggregations or depletions, which result in degraded electric power improvement under a negative temperature difference and upgraded power enhancement under a positive one. At a temperature difference of 30 K, the electric power is enhanced by 56.22% for a thin PET membrane (length = 50 nm) under the negative temperature difference. If the membrane thermal conductivity can be well tuned to nearly thermal insulation, the electric power can be enhanced by 120.07%. To step further, we proposed a criterion for membrane selection based on thermal conductivities in the thermally nanofluidic energy conversion: For thick membranes, materials of large thermal conductivity with a positive temperature difference are preferred for obvious power and energy efficiency enhancement. For thin membranes, materials of small thermal conductivity with a negative temperature difference are appealing. These findings reveal the importance of a long-overlooked factor, membrane thermal conductivity, in nanofluidic energy harvesting and can serve as a guidance for selecting appropriate membrane materials and developing high-performance nanofluidic power devices.

## 1. Introduction

Salinity gradient energy is recognized as a promising candidate for the substitution of traditional fossil fuels [1–4]. Reverse electrodialysis (RED) is developed to capture this energy by converting the Gibbs free energy of mixing into the electric power based on ion exchange membranes (IEMs) that separate salt solutions at different concentrations [5]. However the traditional reverse electrodialysis could not meet the commercial demand for its low power density, mainly hindered by the IEM sub-nanopores [6]. With the development of the nanofabrication and nanotechnology, charged nanopores are employed to function as IEMs, which could provide excellent ion selectivity and ion current [7–10]. The power density of a nanofluidic osmotic energy system can be one to three orders of that based on traditional IEMs [11–14]. Kim et al. obtained a power density 7.7 W/m$^2$ for the RED via a silica nanochannel [15]. And Siria et al. presented a huge high power density over 1000 W/m$^2$ through a single boron nitride nanotube [13].

Most of the researches regarding the nanofluidic energy conversion system focus on fabricating high selectivity membranes with various materials, such as ultrathin Janus membrane [16], single-layer molybdenum disulfide nanopore [17], and oppositely charged graphene oxide membrane pairs [18], as well as adopting asymmetric channel geometries, for instance, hourglass shaped [19],

* Corresponding author.
** Corresponding author.
*** Corresponding author.
*E-mail addresses:* r_long@hust.edu.cn (R. Long), zcliu@hust.edu.cn (Z. Liu), w_liu@hust.edu.cn (W. Liu).

https://doi.org/10.1016/j.nanoen.2019.104284
Received 31 July 2019; Received in revised form 22 October 2019; Accepted 7 November 2019
Available online 12 November 2019
2211-2855/© 2019 Elsevier Ltd. All rights reserved.

conical [20,21], rectangular [22], and cascaded or fractal channels with different pore sizes [23–25]. In addition, the solution properties such as ion type [26], solution pH [27,28] are also introduced to offer a high power density. Cao et al. [29] revealed there exits an optimal channel length leading to the maximum power density for the compromise between the charge selectivity and ion concentration polarization. Recently, attentions have been drawn to investigate the system's temperature dependence. Tseng et al. [30] found the electric power increases with increasing temperature, but the conversion efficiency depends weakly on temperature. However the research is still limited in the isothermal condition, where the salt reservoirs are maintained at the same temperatures [31]. With transmembrane temperature difference applied, heat transfer occurs both through the solid membrane and the salt solution, resulting in *trans*-channel temperature gradients. Due to the Soret effects, ions diffuse along or opposite to the temperature gradient stemming from their different thermal responsiveness [32,33], which could impact the ion transportation characteristics. Previous studies indicate that Sorret effect may be ignorable compared to the impacts of the temperature depended physical properties [34–36]. Recently, we have investigated the electric power under different temperature differences in a thermally insulated nanopore, and found an anomalous temperature depended membrane potential and electric power under the negative/positive temperature difference, where the negative/positive temperature difference is defined as the temperature gradient is in the opposite/same direction of the concentration gradient [36,37]. We have proposed the effects of ionic thermal up-diffusion (enhanced ion diffusion along the osmotic direction under the negative temperature difference) and down-diffusion (weakened ion diffusion along the osmotic direction under the positive temperature difference) to explain such phenomenon. The thermal up-diffusion promotes the selectivity and suppresses the ion concentration polarization (ICP), resulting in enhanced membrane potential and electric power [37]. However, actual materials for fabricating nanopore membranes could not be ideal thermally insulated. The thermal conductivity of conventional materials for nanopore fabrication can be 2 to 3 orders than that of the salty solutions [38], which could significantly impact the temperature distributions in the nanopore, yielding counterintuitive phenomena. Systematical investigations of the heat transfer in the nanofuidic energy harvesting are highly demanded.

In this context, we focus on impacts of the membrane thermal conductivity on the performance of the thermally nanofluidic osmotic energy conversion systems. Heat transfer occurs both in the liquid solution and solid membrane, which impacts the temperature distribution in the nanopore interior and the *trans*-channel ion transportation (Fig. 1). We investigate widely used bulk materials for fabricating nanopores with various thermal conductivities, for instance, polyethylene terephthalate (PET), alumina ($Al_2O_3$), and the silicon nitride ($Si_3N_4$), thus, to provide guidance for selecting appropriate material for membrane fabrication. Under the negative temperature difference, ion diffusion along the osmotic direction is enhanced due to augmented diffusion coefficients, which contributes to ions passing through the nanopore, leading to augmented ionic current and suppressed ICP. Under the positive temperature difference, ion diffusion along the osmotic direction is decreased due to weakened diffusion coefficients, which contributes to ions aggregation in the nanopore and deteriorated ICP. Therefore, the nanofluidic energy conversion system exbibits asymmetric behavior under different temperature differences. Under a positive temperature difference, the electric power shifts from inhibition to promotion as the membrane thermal conductivity increases, while a negative temperature difference always contributes to the electric power (Fig. 1b). Large membrane conductivity evens temperature distribution in the nanochannel, weakening ion aggregation or depletion in the nanopore, resulting in degraded electric power improvement under applied negative temperature difference and upgraded enhancement under the positive one. More intriguingly, at low concentration intensities, the power enhancement under the negative temperature difference overwhelms that under the opposite one due to significantly reversed ion concentration polarization at the high concentration end induced by large membrane thermal conductivity (Fig. 1c). For ion transportation in thick membranes with large thermal conductivities, the Soret effect is found to be not ignorable and can slightly degrade the ion selectivity at a

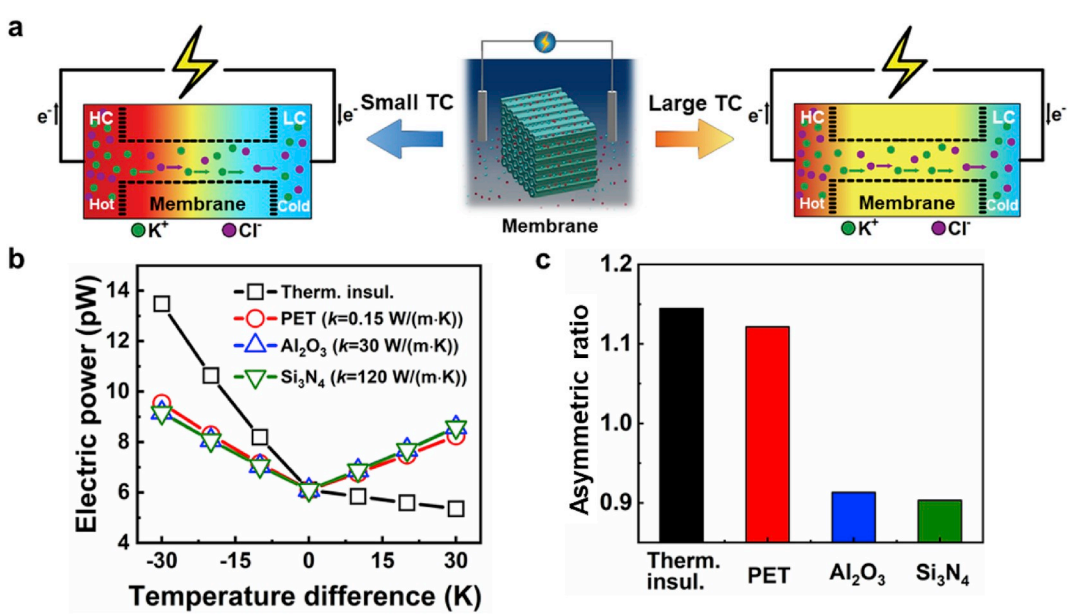


**Fig. 1.** Anomalous thermal conductivity (TC) dependence in thermally nanofluidic energy harvesting system. a) Schematic illustration of the ion and temperature distributions with small and large membrane thermal conductivities with a positive temperature difference applied. b) Electric power under different membrane thermal conductivities and temperature differences. In the calculation, the concentration difference is 1000-fold, the membrane thickness is 50 nm. c) Asymmetric ratio for different membrane thermal conductivities at low concentration intensities. In the calculation, the concentration difference is 1000-fold, the membrane thickness is 5000 nm. The asymmetric ratio is calculated as the power under the negative temperature difference ($T_H = 290$ K, $T_L = 320$ K) dividing that under the positive one of the same magnitudes ($T_H = 320$ K, $T_L = 290$ K), indicating the relative asymmetric power enhancement.

negative temperature difference. In addition, the impacts of the membrane thermal conductivity on the energy efficiency are also discussed. To step further, we proposed a criterion for membrane selection based on thermal conductivities in the thermally nanofluidic energy conversion: For thick membranes, materials of large thermal conductivity with a positive temperature difference are preferred for obvious power and energy efficiency enhancement. For thin membranes, materials of small thermal conductivity with a negative temperature difference are appealing. These findings fill the blank investigation of the membrane thermal conductivity on the nanofluidic performance and can serve as a guidance for selecting appropriate materials for membrane fabrication and employing appropriate temperature differences to enhance the electric power.

## 2. Results and discussion

As the ion selectivity, cation/ation current can not be calculated based on existing methods for postprocessing the experimental data, here, Poisson–Nernst–Planck equations, Navier-Stocks equations and heat transfer equations are employed to illustrate the ion transportation characteristics, thus to give a deep insight into the non-isothermal osmotic energy conversion system. Originating from advances in nanofabrication and nanotechnology, bioinspired or mimic nanochannels can be fabricated. Nanopores with pore sizes of 2–25 nm have been widely investigated in previous literatures regarding the nanofluidic reverse electrodialysis [17]. Therefore, we consider a cylindrical single pore membrane with pore radius $R_n = 8$ nm, at varied length $L_n$ in present study. The membrane with a constant surface charge density of $-0.06 C/m^2$ contacts with two same large reservoirs ($R_r = L_r = 1000$ nm) at different KCl concentrations and temperatures (Fig. S1, Supporting Information). The solution temperature varies from 290 K to 320 K, which can be easily prepared by utilizing the waste heat. $T_H$ denotes the temperature of the high concentration solution and $T_L$ represents that of the low concentration solution. The transmembrane concentration intensity, defined as the concentration difference divided by the nanopore length, is employed to evaluate the ion diffusion strength, which is tuned by varying the channel length from 50 nm to 5000 nm. Kinds of membrane materials are investigated, such as the ideal thermal insulation, PET, $Al_2O_3$, and the $Si_3N_4$ with thermal conductivities at 0 W/(m·K), 0.15 W/(m·K), 30 W/(m·K), 120 W/(m·K), respectively [38]. According to the system configuration, we name the positive temperature difference as that the temperature gradient is in the same direction with the concentration gradient. Hence the negative temperature difference indicates that the temperature gradient direction is opposite to that of the concentration gradient. In the calculation, the osmotic current ($I_{osm}$) is calculated on the short circuit condition, and the membrane potential ($E_{mem}$) is obtained by linear interpolation from different electric currents at varied applied voltages (Fig. S3, Supporting Information). The maximum power reads $P_{max} = I_{osm}\ E_{mem}/4$. The relevant theoretical analysis and the validation of numerical method can be found in the Supporting Information and references therein.

We systematically investigate the impacts of membrane thermal conductivities on the electric power under different concentration intensities and temperature differences (Fig. 2). Here two parameters: enhancement factor and the asymmetric ratio, are employed to quantify the power improvement with asymmetric temperature differences

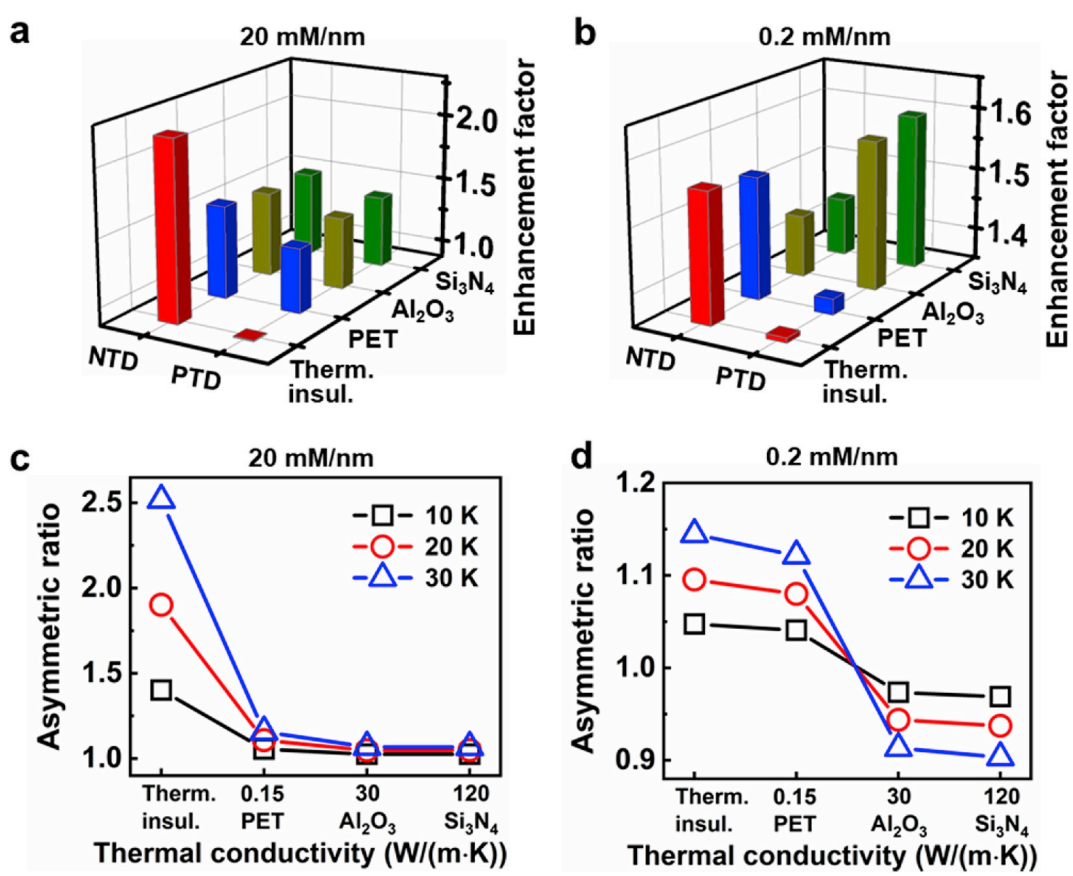


**Fig. 2.** Anomalous membrane thermal conductivity dependence under varied concentration intensities and temperature differences. a, b) Enhancement factor for various membranes under the positive and negative temperature differences. c, d) Asymmetric ratio for various membranes under the positive and negative temperature differences. In the calculation, the concentration intensity is tuned by varying the channel length at a fixed concentration difference (1000-fold). PTD and NTD represent positive temperature difference ($T_H = 320$ K, $T_L = 290$ K) and negative temperature difference ($T_H = 290$ K, $T_L = 320$ K).

involved. The enhancement factor is defined as the electric power obtained with temperature differences diving that under the isothermal condition. And the asymmetric ratio is defined as the power under the negative temperature difference dividing that under the positive one of the same magnitudes, indicating the relative asymmetric power enhancement. A negative temperature difference can significantly increase the electric power, which decreases with increasing membrane thermal conductivities (Fig. S4, Supporting Information). The enhancement factor at a positive temperature difference is sensitively to the membrane conductivity and concentration intensity. At high concentration intensities, for membranes with small thermal conductivities, the enhancement factor is less that one, indicating the electric power is suppressed, which shifts from inhibition to promotion as the membrane thermal conductivity increases. Under small concentration intensities, a positive temperature difference can always enhance the electric power, especially for membranes with larger thermal conductivities (Fig. S5, Supporting Information). The asymmetric ratio decreases with increasing membrane thermal conductivities (Fig. 2c–d, and Fig. S6 in the Supporting Information). Under high concentration intensities, its value is always larger than one, indicating the power improvement under a negative temperature difference is more preferable for thin membranes with small thermal conductivity. Under small concentration intensities, the asymmetric ratio is larger than one for membranes with small thermal conductivities, and is less than one for membranes with large thermal conductivities, revealing that a positive temperature difference is more promising for thick membranes with large thermal conductivity (Fig. 2b).

We further investigate the osmotic current and the membrane potential for various membrane thermal conductivities under different temperature differences and concentration intensities (Fig. 3). Both positive and negative temperature differences are beneficial for the osmotic current, and an anomalous membrane dependence phenomenon occurs (Fig. 3a–d). Under a negative temperature difference, a smaller membrane thermal conductivity leads to a larger osmotic current. While under a positive temperature difference, it exhibits an opposite phenomenon: larger membrane thermal conductivity induces larger osmotic current. The osmotic current is significantly impacted by the thermal up-diffusion that is induced by the negative temperature difference and contributes to the osmotic current, and the thermal down-diffusion, which arises from the positive temperature difference and goes against the osmotic current. A larger membrane thermal conductivity uniforms the temperature distribution in the nanochannel (Fig. S7, Supporting Information), resulting in weakened impacts of the thermal up- and down-diffusion. Thus, the osmotic current for membranes with a large thermal conductivity is enhanced under the positive temperature and is decreased under the negative temperature difference. In addition, a negative temperature difference contributes to the membrane potential, which decreases with increasing membrane thermal conductivities (Fig. 3e–h). Under a positive temperature difference, a small membrane thermal conductivity hinders the membrane potential. However, the membrane potential shifts from inhibition to promotion as the membrane thermal conductivity increases.

The behavior of the membrane potential under different membrane thermal conductivities stems from the compromise of ion selectivity and ion concentration polarization (ICP). At small membrane thermal conductivities, the *trans*-channel temperature gradient is much larger (Fig. 4a). The ion depletion/aggregation induced by the thermal up-/down-diffusion obviously occurs in the nanopore interior, leading to improved/degraded selectivity under the negative/positive temperature differences (Fig. 4b–c). At large membrane thermal conductivities, the *trans*-channel temperature gradient is not obvious, which weakens the effects of the thermal up- and down-diffusion in the nanopore interior. Therefore, the selectivity decreases with increasing membrane thermal conductivities under the negative temperature difference and increases with increasing membrane thermal conductivities under the positive temperature difference (Fig. S8, Supporting Information).

On the other hand, a large membrane thermal conductivity results in obvious temperature gradient in the reservoir zone. Under the positive temperature difference, ions aggregate near the nanopore ends (Fig. 4b), which can greatly improve the local high concentration at the nanopore entrance, leading to enhanced ion concentration in the nanopore, thus to

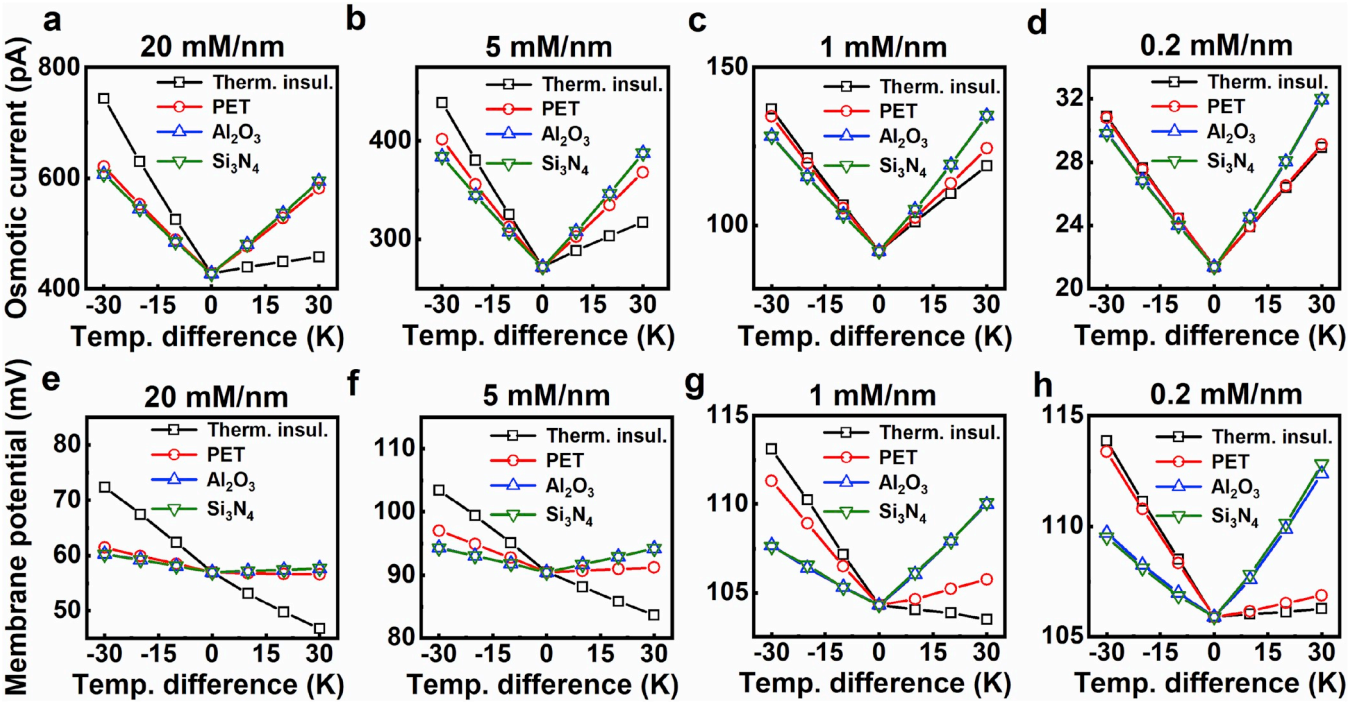


**Fig. 3.** Osmotic current and membrane potential under different membrane thermal conductivities. The concentration intensity is tuned by varying the channel length from 50 nm to 5000 nm at a fixed concentration difference (1000-fold).

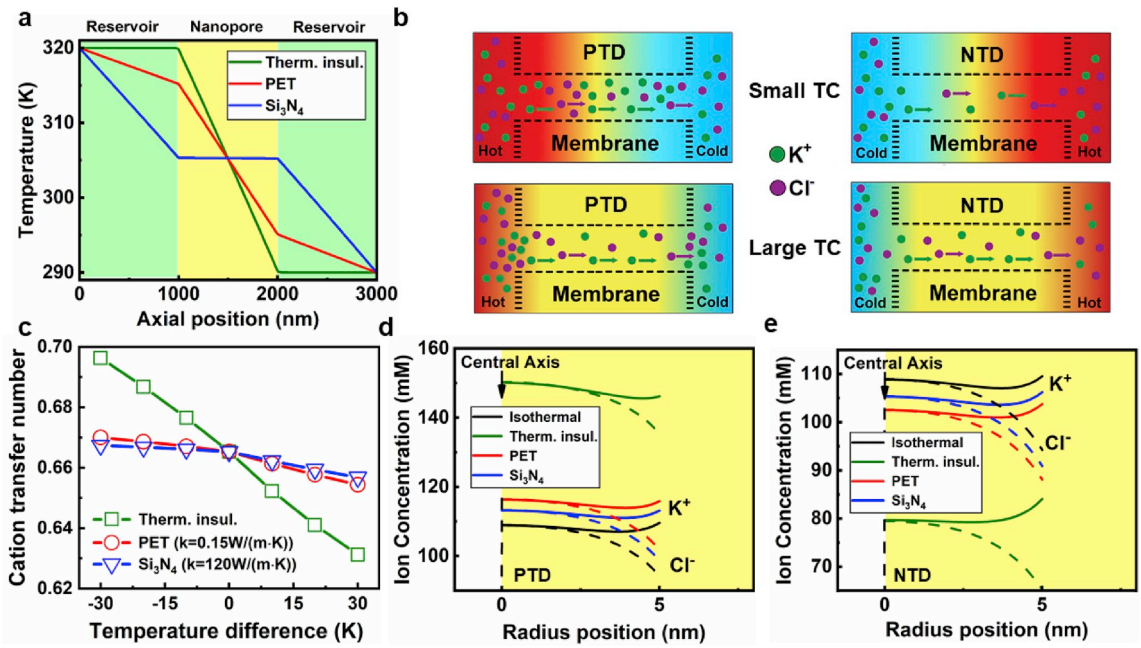


**Fig. 4.** a) Axial temperature distributions under different membrane thermal conductivities. b) Schematic illustration of ion aggregation or depletion for different membrane thermal conductivities and temperature differences. c) Cation transfer number under varied temperature differences at the strong diffusion condition (high concentration intensity). d,e) Radius concentration profiles for cations and anions at cross section at the low concentration exit, where isothermal, PTD, and NTD refers to $T_H = T_L = 290$ K, $T_H = 320$ K and $T_L = 290$ K, and $T_H = 290$ K and $T_L = 320$ K, respectively. In the calculation, the concentration difference is 1000-fold. The membrane thickness is 50 nm.

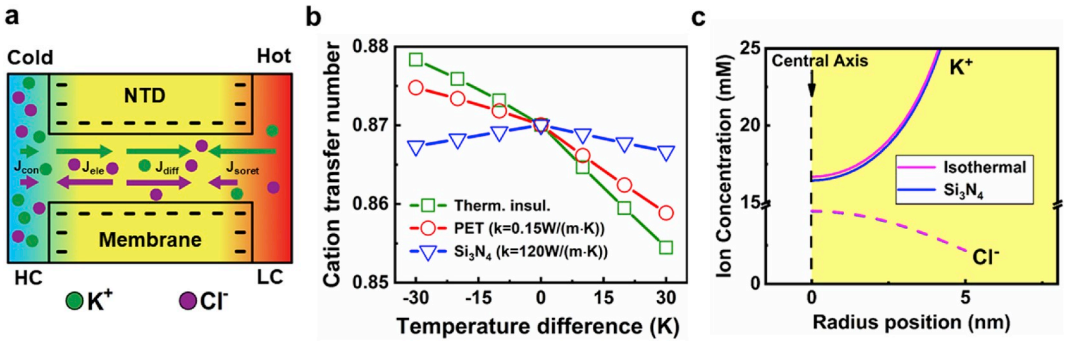


**Fig. 5.** a) Schematic illustration of the impact of Soret effects under the negative temperature difference. b) Cation transfer number under weak diffusion conditions (low concentration intensity). c) Radius concentration profiles for cations and anions at cross section at the low concentration exit under the negative temperature difference ($T_H = 290$ K and $T_L = 320$ K). In the calculation, the concentration difference is 1000-fold and the membrane thickness is 1000 nm.

decrease the electric double layer thickness and worsen the ion selectivity (Fig. S9, Supporting information). The positive temperature difference always degrades the ion selectivity (Fig. S8). More interesting, under low concentration intensities, a negative temperature difference can slightly degrade the ion selectivity for membranes with large thermal conductivities (Fig. 5). The Soret effects induced by the temperature gradient drive the ions to aggregate into the hot or cold sides due to the positive or negative sign of the reduced Soret number, a positive sign of which means the ions (such as $K^+$ and $Cl^-$ in present study) prefer to move towards the cold side. When significant temperature gradients exist in the nanopore interior, the effect of Soret effect can be ignored, compared to the impact of thermal up- or down-diffusion. At lower concentration intensities, the diffusion is weak. Due to evened temperature in the nanopore induced by the large membrane thermal conductivity, the thermal up-diffusion induced by the negative temperature difference is eliminated. The Soret effect comes to act obviously in the reservoirs near the nanopore ends. When a negative temperature difference is applied, $K^+$ and $Cl^-$ at the low concentration end emigrate from the reservoir into the nanopore interior. The ion transportation induced by the Soret effect is opposite to the osmotic direction (Fig. 5a). The reduced Soret coefficient of $K^+$ is much larger than $Cl^-$, indicating $K^+$ migrates more quickly, which decreases the concentration of $K^+$ at the channel exit, resulting in slightly worsened ion selectivity (Fig. 5b–c).

Furthermore, the ICP at the low concentration side is obviously suppressed under negative temperature differences, which improves the effective concentration difference (Fig. 6). Under negative temperature differences both local $C_H$ and $C_L$ are decreased compared to those under the isothermal conditions (Figs. S10 and S11, Supporting Information). The local $C_H$ decreases with increasing membrane thermal conductivities meanwhile the local $C_L$ increases, leading to decreased effective concentration difference (Fig. 6b). A negative temperature difference contributes to the membrane potential due to the coordination of selectivity and ion concentration polarization, which increases with decreasing membrane thermal conductivities. Under positive temperature differences, both local $C_H$ and $C_L$ are increased (Fig. 6b). The local

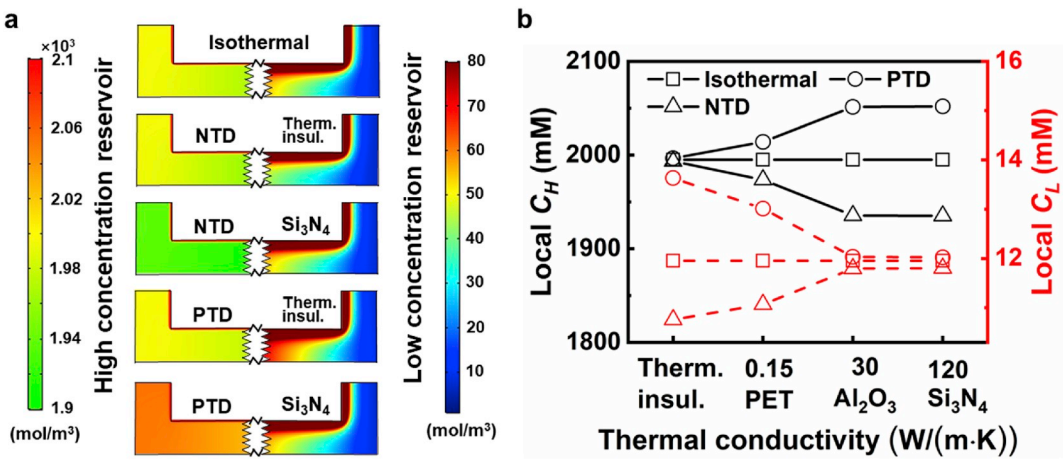


**Fig. 6.** Membrane thermal conductivity depended ion concentration polarization. a) Concentration profiles ($C_K^+ + C_{Cl}^-$) near high and low concentration ends. b) Local concentration near high and low concentration ends. In the calculation, the concentration difference is 1000-fold and the membrane thickness is 1000 nm. Isothermal, PTD, and NTD refers to $T_H = T_L = 290$ K, $T_H = 320$ K and $T_L = 290$ K, and $T_H = 290$ K and $T_L = 320$ K, respectively.

$C_H$ increases with increasing membrane thermal conductivities meanwhile $C_L$ decreases. For membranes with small thermal conductivities, the ICP at the low concentration side strongly exists, leading to degraded effective concentration difference and degraded membrane potential. At large membrane thermal conductivities, an obvious enhancement of local $C_H$ exits, which is much larger than the bulk concentration (Fig. 6b), leading to reversed ion concentration polarization and significantly enhanced effective concentration difference that overrides the impact of the degraded ion selectivity, resulting in elevated membrane potential (Fig. 3).

Based on above considerations, larger membrane thermal conductivity evens temperature distribution in the nanochannel, weakening ion aggregations or depletions, and resulting in degraded electric power improvement under a negative temperature difference and upgraded power enhancement under a positive one. Besides, under the positive temperature difference, at larger thermal conductivities, there exists significant reversed ion concentration polarization at the high concentration end, which increases the effective concentration ratio and enhances the electric power, especially at high concentration intensities, where the power enhancement under the positive temperature difference outnumbers the maximum power enhancement under the negative one.

For the thermally nanofluidic power generation, the energy efficiency is deduced as (Supporting Information)

$$\eta = \frac{(2t_+ - 1)\frac{E_{mem}}{2}}{\frac{R}{F}\ln\frac{\alpha_H^{T_H}}{\alpha_L^{T_L}} + \frac{\Delta\mu_0}{F}} \tag{1}$$

where $\Delta\mu_0$ is the standard chemical potential difference between $T_H$ and $T_L$. $t_+$ is the cation transfer number. Under a negative temperature difference, at high concentration intensities with strong ion diffusion, a larger membrane thermal conductivity is adverse to the energy efficiency for decreased electrical power output (Fig. S12, Supporting information). At low concentration intensities with weak ion diffusion, larger membrane thermal conductivity hinders the effect of the thermal up-diffusion that significantly decreases the transmembrane ions and the Gibbs free energy consumption, leading to augmented energy efficiency, which increases with increasing membrane thermal conductivities, meanwhile the electric power enhancement is degraded. Under the positive temperature difference, as the transmembrane ion diffusion is reduced by the impact of the thermal down-diffusion, the behavior of the energy efficiency exhibits the same behavior with the electric power under various membrane thermal conductivities. The energy efficiency increases with increasing membrane thermal conductivities. At low concentration intensities, the energy efficiency shifts from suppression to augmentation as the membrane thermal conductivity increases. At large membrane thermal conductivities, the energy efficiency under the positive temperature difference overrides that under the negative one due to significantly enhanced electric power. Therefore, for thin membranes, materials of a small thermal conductivity with a negative temperature difference contribute to the energy efficiency. For thick membranes, the energy efficiency for materials of a larger thermal conductivity with a positive temperature difference presents a dominant advantage.

As additional remarks, recently kinds of membranes have been made to improve the osmotic power generation. 2D nanomaterials such as graphene [39], boron nitride [40,41], and molybdenum disulfide [17, 42] have become an active research area of materials science as well as thick bulk materials, for instance, inorganic mica flakes, metal foils, and organic polymer films [43]. Ceramic materials, including alumina, silica, and silicon nitride, are widely employed to construct nanopores for the nanofluidic osmotic energy harvesting [44–46]. Their thermal conductivities vary from nearly zero to hundreds W/(m·K). When the transmembrane temperature difference is imposed, heat transfer occurs in the liquid solution and the solid membrane. The *trans*-channel temperature gradient is significantly impacted by the material thermal conductivity. Present finding may serve as preliminary screening method for material selection based on the material thermal conductivities. For thick membranes, materials of large thermal conductivity with a positive temperature difference are preferred for obvious power and energy efficiency enhancement. For thin membranes, membranes of small thermal conductivity with a negative temperature difference applied are more appealing.

## 3. Conclusion

In conclusion, we systematically investigated the impacts of membrane thermal conductivity on the performance of the thermally nanofluidic energy conversion system, where heat transfer occurs in both the nanopore salt solution and the solid membrane. Under negative temperature differences, membranes with larger thermal conductivities decrease the *trans*-channel temperature gradients, weakening the impact of thermal up-diffusion, leading to degraded power enhancement. Under positive temperature differences, for membranes with a small thermal conductivity, the power is hindered by the significant decrease of membrane potential caused by the thermal down-diffusion. Large membrane thermal conductivity suppresses the *trans*-channel temperature gradients, leading to weakened impact of thermal down-diffusion in

the nanopore, meanwhile it induces reversed ICP at the high concentration end, which increases the effective concentration difference that overriding the impact of degraded ion selectivity, resulting in enhanced electric power. The energy conversion performance via the nanopores fabricated by carefully selected materials can be greatly enhanced when external temperature differences applied. For thick membranes, materials of large thermal conductivity with a positive temperature difference are preferred for obvious power and energy efficiency enhancement. For thin membranes, materials of small thermal conductivity with a negative temperature difference are more appealing. These findings fill the blank investigation of the membrane thermal conductivity on the nanofluidic performance and can serve as a guidance for selecting appropriate materials for membrane fabrication and employing appropriate temperature differences to enhance the electric power.

## Declaration of competing interest

The authors declare no conflict of interest.

## Acknowledgements

This work was financially supported by the National Natural Science Foundation of China (51706076, 51736004).

## Appendix A. Supplementary data

Supplementary data to this article can be found online at https://doi.org/10.1016/j.nanoen.2019.104284.

## References

[1] D. Griggs, M. Staffordsmith, O. Gaffney, J. Rockström, M.C. Ohman, P. Shyamsundar, W. Steffen, G. Glaser, N. Kanie, I. Noble, Nature 495 (2013) 305–307.
[2] L. Wen, L. Jiang, Natl. Sci. Rev. 1 (2013) 144–156.
[3] P. Yang, K. Liu, Q. Chen, J. Li, J. Duan, G. Xue, Z. Xu, W. Xie, J. Zhou, Energy Environ. Sci. 10 (2017) 1923–1927.
[4] L. Qiu, H. Liu, J. Jiang, W. Tan, Natl. Sci. Rev. 5 (2018) 789–791.
[5] B.E. Logan, M. Elimelech, Nature 488 (2012) 313–319.
[6] T. Okada, G. Xie, O. Gorseth, S. Kjelstrup, N. Nakamura, T. Arimura, Electrochim. Acta 43 (1998) 3741–3747.
[7] W. Guo, L. Cao, J. Xia, F.Q. Nie, W. Ma, J. Xue, Y. Song, D. Zhu, Y. Wang, L. Jiang, Adv. Funct. Mater. 20 (2010) 1339–1344.
[8] R. Li, J. Jiang, Q. Liu, Z. Xie, J. Zhai, Nano Energy 53 (2018) 643–649.
[9] S. Qin, D. Liu, Y. Chen, C. Chen, G. Wang, J. Wang, J.M. Razal, W. Lei, Nano Energy 47 (2018) 368–373.
[10] C. Yu, X. Zhu, C. Wang, Y. Zhou, X. Jia, L. Jiang, X. Liu, G.G. Wallace, Nano Energy 53 (2018) 475–482.
[11] W.-J. Lan, M.A. Edwards, L. Luo, R.T. Perera, X. Wu, C.R. Martin, H.S. White, Accounts Chem. Res. 49 (2016) 2605–2613.
[12] T.B.H. Schroeder, A. Guha, A. Lamoureux, G. VanRenterghem, D. Sept, M. Shtein, J. Yang, M. Mayer, Nature 552 (2017) 214.
[13] A. Siria, P. Poncharal, A.-L. Biance, R. Fulcrand, X. Blase, S.T. Purcell, L. Bocquet, Nature 494 (2013) 455.
[14] J. Gao, X. Liu, Y. Jiang, L. Ding, L. Jiang, W. Guo, Small 15 (2019) 1804279.
[15] D.-K. Kim, C. Duan, Y.-F. Chen, A. Majumdar, Microfluid. Nanofluidics 9 (2010) 1215–1224.
[16] Z. Zhang, X. Sui, P. Li, G. Xie, X.Y. Kong, K. Xiao, L. Gao, L. Wen, L. Jiang, J. Am. Chem. Soc. 139 (2017) 8905.
[17] J. Feng, M. Graf, K. Liu, D. Ovchinnikov, D. Dumcenco, M. Heiranian, V. Nandigana, N.R. Aluru, A. Kis, A. Radenovic, Nature 536 (2016) 197.
[18] J. Ji, Q. Kang, Y. Zhou, Y. Feng, X. Chen, J. Yuan, W. Guo, Y. Wei, L. Jiang, Adv. Funct. Mater. 27 (2017).
[19] Z. Huacheng, H. Xu, H. Jue, Z. Lu, T. Ye, L. Lin, J. Lei, Adv. Funct. Mater. 25 (2015) 1102–1110.
[20] J. Cervera, A. Alcaraz, B. Schiedt, a.R. Neumann, P. Ramírez, J. Phys. Chem. C 111 (2007) 12265.
[21] H.C. Yeh, C.C. Chang, R.J. Yang, RSC Adv. 4 (2013) 2705–2714.
[22] W. Jung, J. Kim, S. Kim, H.G. Park, Y. Jung, C.-S. Han, Adv. Mater. 29 (2017) 1605854.
[23] J. Gao, W. Guo, D. Feng, H. Wang, D. Zhao, L. Jiang, J. Am. Chem. Soc. 136 (2014) 12265.
[24] R. Long, Z. Kuang, Z. Liu, W. Liu, Phys. Chem. Chem. Phys. 20 (2018) 7295–7302.
[25] Z. Kuang, D. Zhang, Y. Shen, R. Long, Z. Liu, W. Liu, J. Power Sources 418 (2019) 33–41.
[26] J. Hwang, S. Kataoka, A. Endo, H. Daiguji, Lab Chip 16 (2016) 3824–3832.
[27] Y. Ma, L.H. Yeh, C.Y. Lin, L. Mei, S. Qian, Anal. Chem. 87 (2015) 4508–4514.
[28] L.H. Yeh, F. Chen, Y.T. Chiou, Y.S. Su, Small 13 (2017) 1702691.
[29] L. Cao, F. Xiao, Y. Feng, W. Zhu, W. Geng, J. Yang, X. Zhang, N. Li, W. Guo, L. Jiang, Adv. Funct. Mater. 27 (2017) 1604302.
[30] S. Tseng, Y.-M. Li, C.-Y. Lin, J.-P. Hsu, Nanoscale 8 (2016) 2350–2357.
[31] J. Hwang, T. Sekimoto, W.-L. Hsu, S. Kataoka, A. Endo, H. Daiguji, Nanoscale 9 (2017) 12068–12076.
[32] A. Würger, Phys. Rev. Lett. 101 (2008) 108302.
[33] D. Vigolo, R. Rusconi, H.A. Stone, R. Piazza, Soft Matter 6 (2010) 3489–3493.
[34] J.A. Wood, A.M. Benneker, R.G. Lammertink, J. Phys. Condens. Matter 28 (2016) 114002.
[35] A.M. Benneker, H.D. Wendt, R.G.H. Lammertink, J.A. Wood, Phys. Chem. Chem. Phys. 19 (2017) 28232–28238.
[36] R. Long, Z. Kuang, Z. Liu, W. Liu, J. Membr. Sci. 561 (2018) 1–9.
[37] R. Long, Z. Kuang, Z. Liu, W. Liu, Natl. Sci. Rev. (2019), https://doi.org/10.1093/nsr/nwz106.
[38] H. Chen, V.V. Ginzburg, J. Yang, Y. Yang, W. Liu, Y. Huang, L. Du, B. Chen, Prog. Polym. Sci. 59 (2016) 41–85.
[39] J. Wilson, L. Sloman, Z. He, A. Aksimentiev, Adv. Funct. Mater. 26 (2016) 4830.
[40] D. Golberg, Y. Bando, Y. Huang, T. Terao, M. Mitome, C. Tang, C. Zhi, ACS Nano 4 (2010) 2979.
[41] A. Siria, P. Poncharal, A.L. Biance, R. Fulcrand, X. Blase, S.T. Purcell, L. Bocquet, Nature 494 (2013) 455–458.
[42] M.C. Yu, Y.Y. Xin, L. Zhen, U. Paik, W.L. Xiong, Sci. Adv. 2 (2016), e1600021.
[43] J. Gierak, A. Madouri, A.L. Biance, E. Bourhis, G. Patriarche, C. Ulysse, D. Lucot, X. Lafosse, L. Auvray, L. Bruchhaus, Microelectron. Eng. 84 (2007) 779–783.
[44] S. Wu, F. Wildhaber, A. Bertsch, J. Brugger, P. Renaud, Appl. Phys. Lett. 102 (2013) 2274.
[45] S. Wu, F. Wildhaber, O. Vazquezmena, A. Bertsch, J. Brugger, P. Renaud, Nanoscale 4 (2012) 5718–5723.
[46] Z. Zhang, L. Wen, L. Jiang, Chem. Soc. Rev. 47 (2018) 322–356.

**Rui Long** is an assistant professor of the School of Energy and Power Engineering, Huazhong University of Science and Technology (HUST). He received his Bachelor degree (2011) and Doctoral degree (2016) in HUST. His research interests focus on energy system development and optimization for renewable energy and low-grade heat, nanofluidic energy conversion and ion transportation, as well as thermal management of electronic devices and systems. He has authored and co-authored about 40 research papers included in SCI.

**Zuoqing Luo** is a master degree candidate in School of Energy and Power Engineering, Huazhong University of Science and Technology (HUST). Afer receiving his Bachelor's degree in Harbin Engineering University (HEU) in 2019, he is now supervised by Rui Long in HUST. His research mainly focuses on nanofluidic energy conversion and ion transportation.

**Zhengfei Kuang** is a master degree candidate in the School of Energy and Power Engineering, Huazhong University of Science and Technology (HUST). He received his Bachelor degree (2017) in HUST. He is now supervised by Rui Long in HUST. His research focuses on nanofluidic energy conversion and ion transportation. He has published 5 research papers included in SCI.

**Zhichun Liu** is a professor in the School of Energy and Power Engineering, Huazhong University of Science and Technology of China (HUST). He received his Ph.D. from HUST in 2006, and was visiting scholar in Massachusetts Institute of Technology, US in 2012. His research focuses on heat transfer in nanoscale, electronic cooling, porous media and energy conservation. He published 66 academic papers included in SCI.

**Wei Liu** is a professor of the School of Energy and Power Engineering, Huazhong University of Science and Technology. He has been engaged in teaching and research of heat transfer, energy conservation, electronic cooling, and porous media. He published two textbooks, three academic monographs, and 220 academic papers included in SCI. His H factor is 50. He also authorized 16 national invention patents. He enjoys the government subsidy of the State Council. He is member of the China Society of Engineering Thermophysics, and former director of China Renewable Energy Society.